ACS EARTH AND SPACE CHEMISTRY

Article

Cite This: ACS Earth Space Chem. 2019, 3, 413−423

http://pubs.acs.org/journal/aesccq

Effect of the Hydroxyl Group on Yields and Composition of Organic Aerosol Formed from OH Radical-Initiated Reactions of Alcohols in the Presence of NO_x

Lucas B. Algrim[†,‡] and Paul J. Ziemann*[,†,‡]

[†]Department of Chemistry, University of Colorado, Boulder, Colorado 80309, United States

[‡]Cooperative Institute for Research in Environmental Sciences (CIRES), Boulder, Colorado 80309, United States

Supporting Information

ABSTRACT: The effect of a hydroxyl group and its position on the yields of secondary organic aerosol (SOA) formed from OH radical-initiated reactions of the 1- to 5-decanol isomers, 1- and 2-undecanol isomers, and *n*-decane in the presence of NO_x was investigated in a series of environmental chamber experiments. SOA composition was also measured using liquid chromatography, mass spectrometry, and infrared spectroscopy, and gas-phase aldehydes were measured using gas chromatography and proton transfer reaction−mass spectrometry. It was observed that all decanol isomers formed SOA of a similar composition, which consisted of products similar to those known to be formed from the reaction of *n*-decane but with an added hydroxyl or keto group. SOA yields measured for the decanol isomers were all higher than the yield from *n*-decane because of the general lowering of product vapor pressures by the added hydroxyl group, but they decreased monotonically as the hydroxyl group moved from the end of the molecule to the middle. This isomeric trend can be explained by the effect of the position of the hydroxyl group on the fraction of first-generation products formed through pathways involving alkoxy radical isomerization and is consistent with the yields of these products estimated using a kinetics model. Products formed by these pathways tend to have low volatility and, thus, partition into particles, whereas products formed by the major competing pathways are more volatile. The results demonstrate the need to understand not only the effect of functional groups on volatility but also the effect of their location on volatile organic compound oxidation products and mechanisms to accurately predict SOA yields.

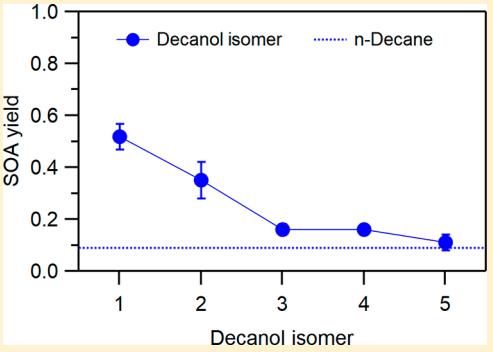

KEYWORDS: *volatile organic compounds, secondary organic aerosol, alkoxy radicals, functionalization, fragmentation*

INTRODUCTION

Volatile organic compounds (VOCs) are emitted into the atmosphere from biogenic and anthropogenic sources in amounts in excess of 1000 TG a year.[1] While these VOCs are generally emitted in a reduced form, in the oxygen-rich atmosphere they can undergo chemical processing that alters their structure by adding functional groups and breaking C−C bonds.[2] If the volatility of a compound is reduced sufficiently in this process, it can condense onto a pre-existing particle, thereby forming secondary organic aerosol (SOA). Studies of SOA have been largely motivated by the significant contribution that it makes to fine particulate matter,[3] which, in turn, impacts visibility, climate processes, and human health.[4]

Because urban SOA is largely formed from anthropogenic VOCs, it can potentially be abated through air quality regulations. In the past, it was thought that most of this material was formed from VOCs emitted from motor vehicles,[5,6] in particular unburned gasoline and diesel fuel.[7] However, studies have also indicated that partially oxidized fuel components, which are thought to contribute to a complex mixture of unspeciated compounds (i.e., compounds that are not resolved by gas chromatography) present in vehicle exhaust, may also be important precursors for SOA formation.[6,8] In addition, a recent study has indicated that volatile chemical products (VCPs) consisting of hydrocarbons and oxygenated organic compounds that are present (often as solvents) in products used by industry and consumers can also serve as SOA precursors.[9] Because of the exponential decrease in vehicle emissions[10] that has resulted from decades of policy implementation and improved engineering (catalytic converters and fuel reformulations), VCPs may now be of greater importance for SOA formation than vehicle emissions.

Given the potential importance of oxygenated organic compounds to vehicle and VCP emissions and SOA formation, a more thorough understanding of the atmospheric chemistry and fate of these compounds is needed. One such class of

Received: January 12, 2019
Revised: February 14, 2019
Accepted: February 15, 2019
Published: February 15, 2019

DOI: 10.1021/acsearthspacechem.9b00015
ACS Earth Space Chem. 2019, 3, 413−423

compounds is alcohols. Although studies have been conducted on small saturated and unsaturated alcohols to determine the products and mechanisms of oxidation[11−13] as well as SOA yields,[14] to our knowledge, the only studies on larger alcohols that have the potential to form significant amounts of SOA were those conducted on glycol ethers because of their use in consumer products.[15] Here, we reacted a series of decanol positional isomers with OH radicals in the presence of NO_x to determine the effect of a hydroxyl group and its location on SOA yields and composition. The approach allows for the results to be interpreted in terms of the effect of the molecular structure on key reaction pathways and product volatility and is similar to the approach that we used recently[16] to determine the effect of a keto group and its location on these SOA properties.

EXPERIMENTAL SECTION

Chemicals. The following chemicals were used: 1-decanol (99%), 2-decanol (96%), 3-decanol (99%), 4-decanol (98%), 5-decanol (97%), 5-undecanol (95%), and 6-undecanol (95%) from Chemsampco, bis(2-ethylhexyl) sebacate (DOS, 97%) from Fluka, acetonitrile (HPLC grade, ACS) from Fisher, and NO (99%) from Matheson. Methyl nitrite was synthesized[17] and stored in a lecture bottle until used. The purity determined periodically by infrared spectroscopy was 99%.

Environmental Chamber Experiments. Experiments were conducted in an 8.0 m^3 FEP Teflon environmental chamber in Boulder, CO, that was filled with clean, dry air [<5 ppb of hydrocarbons and <1% relative humidity (RH)] from two Aadco clean air systems and operated at ambient temperature (~23 °C) and pressure (~630 Torr). In a typical experiment, a VOC (decanol, undecanol, or *n*-decane) was added to the chamber by evaporating a measured amount of the compound from a heated glass bulb into a stream of ultrahigh-purity (UHP) N_2. Approximately 200 $\mu g\ m^{-3}$ dioctyl sebacate (DOS) seed particles in UHP N_2 were added from an evaporation−condensation apparatus. Known amounts of methyl nitrite and NO were prepared on a vacuum manifold using a calibrated glass bulb and absolute pressure gauge and then flushed into the chamber with UHP N_2. Reactions were initiated by turning on blacklights that covered two walls of the chamber at 50% intensity (J_{NO_2} = 0.37 h^{-1}) for 1 h or 100% intensity (J_{NO_2} = 0.61 h^{-1}) for 1 min. Photolysis of methyl nitrite created OH radicals[18] with average concentrations of 2 × 10^8 and 4 × 10^7 molecules cm^{-3} for the 1 min and 1 h reactions, respectively, as determined from the measured decay of the VOC and estimated OH reaction rate constants.[19] The VOC, methyl nitrite, and NO concentrations were 1, 5, and 5 ppm for the 1 h irradiations and 2, 10, and 10 ppm for the 1 min irradiations, respectively. Reported SOA yields were all determined in the experiments with 1 h of irradiation.

Gas Analysis. Air was sampled from the environmental chamber through a glass tube packed with a Tenax TA solid adsorbent at 0.25 L min^{-1} for 4 min to collect VOCs for analysis by gas chromatography with flame ionization detection (GC−FID). While this adsorbent collects both gases and particles, the VOCs of interest should only have been present in the gas phase. Replicate samples were collected 90 and 30 min before reaction and then 30 and 90 min after reaction to verify that the parent VOC concentration was essentially constant and, thus, had established gas−wall partitioning equilibrium. The VOCs adsorbed to the Tenax were thermally desorbed inside a HP 6890 GC−FID equipped with a DB-1701 column (30 m × 0.530 mm with 1 μm film thickness) by heating the inlet to 250 °C in 7 min, while the column was held at 40 °C, and then the column temperature was ramped at 10 °C min^{-1} to 280 °C.

In some experiments, a proton transfer reaction−mass spectrometer (PTR−MS) equipped with a quadrupole mass spectrometer was used to analyze organic gases in the chamber throughout the experiment. The PTR−MS employs H_3O^+ as a reagent ion to chemically ionize any VOC with a proton affinity greater than water via proton transfer.[20] Although, for most compounds, a $[M + H]^+$ ion is formed, alcohols will often lose water to form a $[M + H - H_2O]^+$ ion (m/z 141 for decanol). In the experiments in which the PTR−MS was operated, measurements made for extended periods before and after reaction confirmed that the decanol concentration was essentially constant and, thus, that decanol had achieved gas−wall partitioning equilibrium. Furthermore, PTR−MS measurements of the amount of decanol reacted were within ±10% of the values determined from GC−FID analysis. The GC−FID measurements were used to calculate SOA yields because they were determined in every experiment. Concentrations of NO were monitored with a calibrated Thermo Environmental Instruments 42C NO−NO_2−NO_x analyzer.

Particle Analysis. The composition of particles was monitored in real time during each experiment using a thermal desorption particle beam mass spectrometer (TDPBMS).[21] In this instrument, the particles are focused into a beam in an aerodynamic lens, transported into a high vacuum region, and impacted onto a coated copper rod that is resistively heated to 160 °C. Resulting vapors are ionized by electrons and detected with a triple-quadrupole mass spectrometer. Particle size distributions were measured with a scanning mobility particle sizer (SMPS) and used to calculate aerosol volume concentrations.[22]

After each experiment, aerosol was collected on pre-weighed Teflon filters (0.45 μm pore size) by sampling at 14 L min^{-1} for 90 min. Filters were reweighed to determine the aerosol mass; the aerosol was extracted by rinsing filters with 4 mL of ethyl acetate 3 times; and then the extracts were combined and dried in a stream of UHP N_2. The dried extract was weighed, then reconstituted in acetonitrile, and stored in a freezer at −25 °C until further use. The mass of aerosol extracted was on average within ±4% of the on-filter mass, indicating that extraction efficiencies were close to 100%. Filter and extracted mass was also on average within ±6% of the mass predicted to be collected on filters based on SMPS measurements made during sampling, providing additional support for the accuracy of values used to calculate SOA yields.

The SOA/acetonitrile solution was analyzed by reversed-phase high-performance liquid chromatography (HPLC) using a Shimadzu HPLC equipped with an Agilent Zorbax Eclipse Plus XDB-C_{18} column (250 × 4.6 mm with 5 μm particle size). A binary phase solvent gradient was started at 100% solution A (5% acetonitrile in water) and ramped to 60% A at 2.0% min^{-1} and then from 60 to 0% A at 1.5% min^{-1}, where it was held for 20 min. Solution B, which made up the remainder of the mobile phase, was pure acetonitrile. Compound absorbance by nitrate groups was measured at 210 nm with an ultraviolet/visible (UV/vis) diode array detector.

HPLC peaks from selected analyses were collected as fractions and analyzed in either a Thermo PolarisQ chemical ionization−ion trap mass spectrometer (CI−ITMS) equipped

DOI: 10.1021/acsearthspacechem.9b00015
ACS Earth Space Chem. 2019, 3, 413−423

Scheme 1. Proposed Mechanism for Forming First-Generation Products from the Reaction of 3-Decanol with OH Radicals in the Presence of NO_x[a]

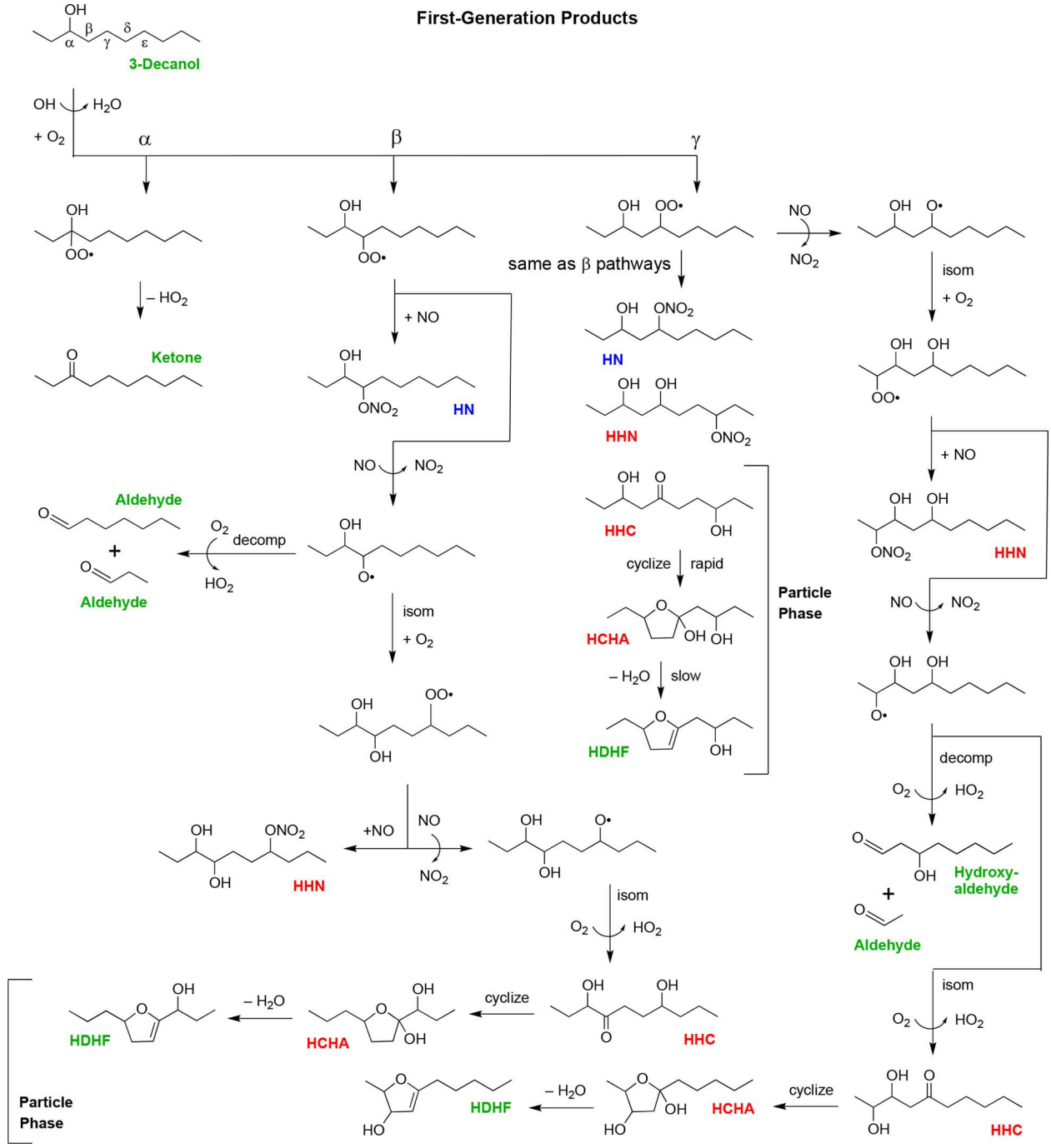

[a]Products highlighted in red are predicted to be >90% in the particle phase; those in green are predicted to be >90% in the gas phase; and those in blue are predicted to be in both phases. The brackets refer to reactions that occur in the particle phase. Mass spectra of SOA indicate the presence of HHN and HCHA products.

with a direct insertion probe for thermal desorption of samples[23] or an Agilent Cary 630 attenuated total reflectance Fourier transform infrared spectrometer (ATR−FTIR). The CI−ITMS was operated in positive mode with isobutane as the reagent gas, which results primarily in protonated molecular ions and their fragment ions. The ATR−FTIR is equipped with a diamond crystal and was operated at 4 cm^{-1} resolution. For each ATR−FTIR analysis, a background spectrum was collected using the same settings and subtracted from the sample spectrum.

SOA Yields. SOA mass yields were calculated for each reaction as the mass of SOA formed divided by the mass of VOC reacted.[24] The mass of SOA formed was determined from SMPS measurements of the aerosol volume concentration, which reached a maximum 20−40 min into each 60 min reaction and then slowly decreased as a result of the loss of particles to the walls. The measurements were corrected for

DOI: 10.1021/acsearthspacechem.9b00015
ACS Earth Space Chem. 2019, 3, 413−423

particle wall losses up to the time that the maximum was reached using the decay of the DOS m/z 185 signal monitored with the TDPBMS. Because DOS is essentially non-volatile, its decay during an experiment (~10% h^{-1}) could be fully attributed to the loss of particles to the walls. The DOS loss rate was thus used to calculate the aerosol volume lost to walls during each full 4.2 min SMPS scan until the maximum was reached, and then these values were added to the maximum measured aerosol volume. The initial DOS volume was subtracted from the wall-loss-corrected aerosol volume to obtain the SOA volume, which was then multiplied by an appropriate density for this SOA of 1.1 g cm^{-3},[25] to obtain the mass of SOA formed. This approach for correcting for particle wall loss should be reasonably accurate because particle diameters grew to >200 nm within a few minutes of turning on the lights, and for particles of this size, the effect of the particle size on wall loss is minor.[26]

The mass of VOC reacted was determined from the GC−FID analyses. Measurements made before reactions were initiated indicated that no *n*-decane and 15−20% of added alcohol had partitioned to the chamber walls, consistent with past measurements.[27] However, because the time-dependent Tenax and PTR−MS measurements indicated that the VOCs had achieved gas−wall partitioning equilibrium before and after the reaction, no correction for partitioning was necessary to determine the mass of VOC reacted. As shown previously,[28] in this case the concentration of reacted VOC is $[VOC]_{reacted} = [VOC]_{T,i}(1 - FID_f/FID_i)$, where $[VOC]_{T,i}$ is the mass of added VOC divided by the chamber volume and FID_i and FID_f are the FID signals/volume of sampled air measured before and after reaction, respectively.

No attempt was made to correct the SOA yields for gas−wall partitioning of reaction products, which has been shown to occur in environmental chamber experiments.[29−31] However, because most of the products that contribute to SOA partition almost entirely to the particle phase (Table S1 of the Supporting Information) on time scales of a few seconds at these high mass loadings, the wall loss of vapors should be minor. Furthermore, because the composition of the SOA is shown to be similar for these decanol isomers, the effects of gas−wall partitioning should be similar for the compounds investigated. Last, because the major focus of this study is on the trends in SOA yields across the range of isomers rather than the absolute yields, gas−wall partitioning should not significantly affect the interpretation of the results.

RESULTS AND DISCUSSION

Mechanism of the Reaction of Decanol with OH Radicals in the Presence of NO_x. The mechanism of the reaction of decanol with OH radicals in the presence of NO_x is similar to that of a *n*-alkane (a linear alkane), which is reasonably well-understood.[19] Although decanol reacts faster with OH radicals than *n*-decane because of the activating effect of the hydroxyl group, the reactivity does not vary significantly among the decanol positional isomers. The mechanism of the reaction is shown in Scheme 1, where 3-decanol is used as an example. Because this mechanism is meant to be applicable to all isomers and many of the products have the same distribution of functional groups, for the sake of simplicity, we do not designate products according to the locations of functional groups. Because of the special importance of certain hydroxyalkoxy radicals, however, we do specify the relationship among functional groups for that species when useful.

The reaction is initiated by abstraction of an H atom along the carbon chain to form H_2O and an alkyl radical, which reacts solely by the addition of O_2 to form an alkylperoxy radical. Abstraction of the H atom on the hydroxyl group is negligible.[32] The location of abstraction relative to the hydroxyl group significantly influences the products formed. The reaction at the β-carbon leads to the most complex set of reactions and is described first in detail to demonstrate the primary reaction pathways that can occur for all isomers. Abstraction of a H atom at the β-carbon results in the formation of a β-hydroxyperoxy radical. In the presence of NO_x, the β-hydroxyperoxy radical reacts with NO to form a β-hydroxynitrate (HN) or a β-hydroxyalkoxy radical and NO_2. The β-hydroxyalkoxy radical will decompose or isomerize, with decomposition and subsequent reaction with O_2 leading to HO_2 and a pair of aldehydes. Isomerization of the β-hydroxyalkoxy radical occurs via a 1,5-H shift to form a dihydroxyalkyl radical, which adds O_2 to form a dihydroxyperoxy radical. This radical then reacts with NO to form a dihydroxynitrate (HHN) or a dihydroxyalkoxy radical, which isomerizes via a reverse 1,5-H shift to form a trihydroxyalkyl radical that then primarily reacts with O_2 to form HO_2 and a dihydroxycarbonyl (HHC). Isomerization via a 1,6-H shift can also occur, but because this is a minor pathway specific to the reaction initiated at the β-carbon, it is not shown in Scheme 1. Furthermore, because the dihydroxyalkoxy radical does not have a hydroxyl group adjacent to the alkoxy group (as do β-hydroxyalkoxy radicals), the rate of decomposition is dramatically reduced and it only isomerizes.[33,34] Upon colliding with particles, HHC rapidly cyclize to hydroxy-cyclic hemiacetals (HCHA), which are expected to be the only significant form of these products.[35] HCHA can then undergo relatively slow acid-catalyzed dehydration to form more volatile hydroxy-dihydrofurans (HDHF), with HNO_3 formed from the NO_2 + OH reaction acting as the catalyst.[36]

The mechanisms of reactions initiated by H atom abstraction at α- and γ-carbons are also shown in Scheme 1. These pathways are similar to those described above and lead to a ketone (aldehyde for 1-decanol) and HN, HHN, and HHC (which cyclize in particles to HCHA and then possibly dehydrate to form HDHF), respectively. Note that, for reaction at the γ-carbon, the γ-hydroxyalkoxy radical can not only isomerize by a 1,5-H shift further along the carbon chain, similar to the pathway shown for β-hydroxyalkoxy radicals, but also isomerize across the hydroxyl group (right-hand pathway in Scheme 1). Similarly, for reaction at δ- and ε-carbons (labeled in Scheme 1 but without reactions shown), the δ- and ε-hydroxyalkoxy radicals can isomerize in both directions. For the δ-hydroxyalkoxy radical, isomerization toward the hydroxyl group occurs by H atom abstraction from the α-carbon and is followed by reaction with O_2 to form HO_2 and a hydroxycarbonyl (which will cyclize in particles to a CHA and then possibly dehydrate to form a DHF). For the ε-hydroxyalkoxy radical, isomerization toward the hydroxyl group can lead to the formation of a β-hydroxyalkoxy radical and thus enhanced decomposition. The hydroxyl group does not influence the mechanisms of reactions that are initiated by abstraction of H atoms at carbons beyond the ε-carbon. The relative importance of each of the 10 H atom abstraction pathways was estimated using structure−reactivity relationships[19] and are given in Table S1 of the Supporting Information.

DOI: 10.1021/acsearthspacechem.9b00015
ACS Earth Space Chem. 2019, 3, 413−423

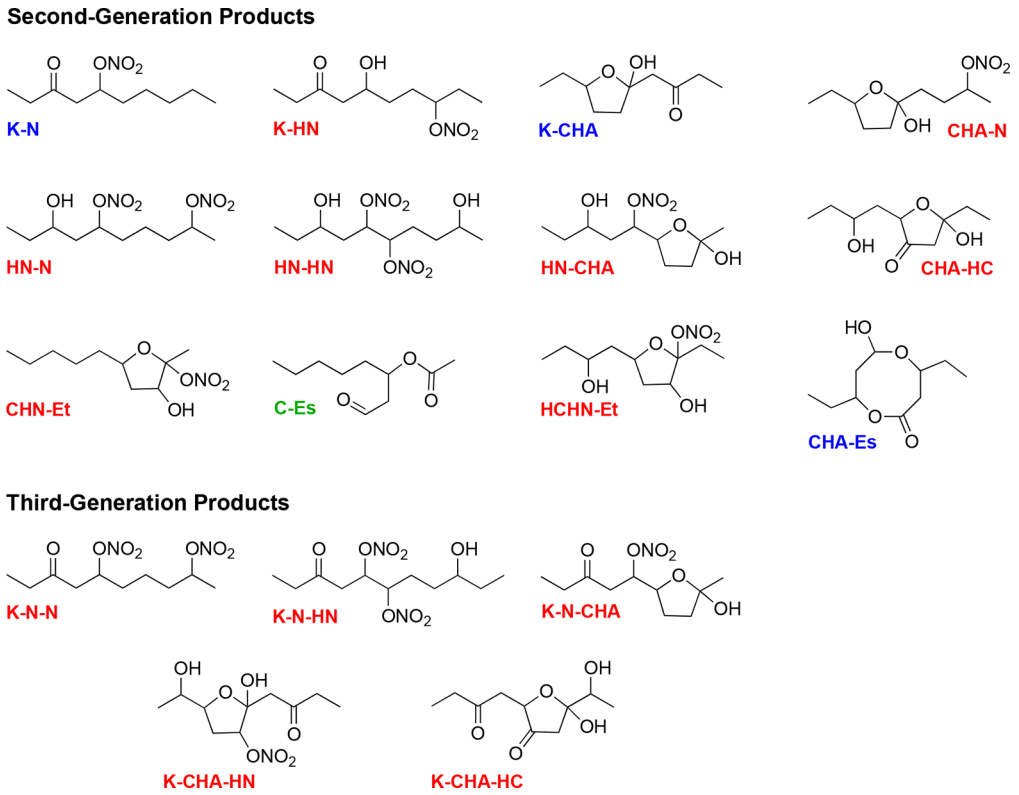

Figure 1. Proposed major second-generation products formed from the reaction of 3-decanol with OH radicals in the presence of NO_x. Products highlighted in red are predicted to be >90% in the particle phase; those in green are predicted to be >90% in the gas phase; and those in blue are predicted to be in both phases.

The vapor pressures of products and the aerosol mass loading determine the extent to which products will partition to particles (a process that will occur on the order of seconds in these experiments) or remain in the gas phase. Color coding in Scheme 1 and Figure 1 classifies the phase of each product as predominantly gas, gas and particle, or particle based on calculations performed using SIMPOL.1[37] and gas−particle partitioning theory,[38] with numerical values given in Table S2 of the Supporting Information. The first-generation ketone, HN, and HDHF products in Scheme 1 (as well as CHA and DHF not shown) are sufficiently volatile that they can react with OH radicals in the gas phase to form the second-generation products shown in Figure 1, whereas HHN and HCHA exist almost entirely in the particle phase and, therefore, do not react further. Reactions of aldehydes are expected to mostly form products via decomposition that are too volatile to form SOA and, therefore, are not included in the figure. Ketone (K), HN, and CHA will react by the same H atom abstraction pathways described above to mostly form products that are similar to first-generation products but with additional N, HN, and HC groups (with the HC cyclizing in particles to a CHA, unless a strained bicyclic structure is formed). These products are shown in Figure 1: K−N, K−HN, K−CHA, HN−N, HN−HN, HN−CHA, CHA−N, and CHA−HC. Note that some reactions lead to the same types of products, which are not shown twice. DHF and HDHF will react even more quickly, primarily by the addition of OH the C═C double bond. Major products from the DHF reaction are a cyclic hydroxynitrate ether (CHN−Et) and a carbonyl ester (C−Es), and major products from the HDHF reaction are a HCHN-Et and hydroxycarbonyl ester that cyclizes in particles to a cyclic hemiacetal ester (CHA−Es). Note that CHN−Et and HCHN−Et are not cyclic hemiacetals but isomers in which the hydroxyl and nitrate groups are switched because the formation of tertiary β-hydroxyalkyl radicals is strongly preferred when OH radicals add to the HDHF C═C double bond.[39] Second-generation K−N and K−CHA products are also sufficiently volatile that they can further react with OH radicals in the gas phase by the addition of N, HN, and HC groups (with HC cyclizing in particles to a CHA, unless a strained bicyclic structure is formed) to form third-generation K−N−N, K−N−HN, K−N−CHA, K−CHA−HN, and K−CHA−HC products (Figure 1), whereas the other second-generation products exist almost entirely in the particle phase and, therefore, do not react further.

Particle-Phase Products. The mass spectra of SOA typically evolved over the first few minutes of a reaction as first- and then second-generation products were formed but then changed relatively little over the remainder of the reaction. For this reason, mass spectra averaged over the 1 h reaction of each decanol isomer are shown in Figure 2. With the exception of 1-decanol, they are similar. The difference for 1-decanol could be due to different chemistry that occurs when the hydroxyl group is on the terminal carbon but is more likely due to different electron ionization fragmentation pathways of primary and secondary alcohols.[40] This explanation is supported by the similar HPLC−UV/vis chromatograms of nitrate-containing products in SOA formed from reactions of all of the isomers, which are shown in Figure 3A.

In all of the isomer mass spectra, significant peaks are present at m/z 153, 169, 171, 199, 216, 218, 230, 232, 246, and 260 that can be assigned to fragment ions that are characteristic of first-, second-, and third-generation products that are expected to be present to a large extent in particles

DOI: 10.1021/acsearthspacechem.9b00015
ACS Earth Space Chem. 2019, 3, 413−423

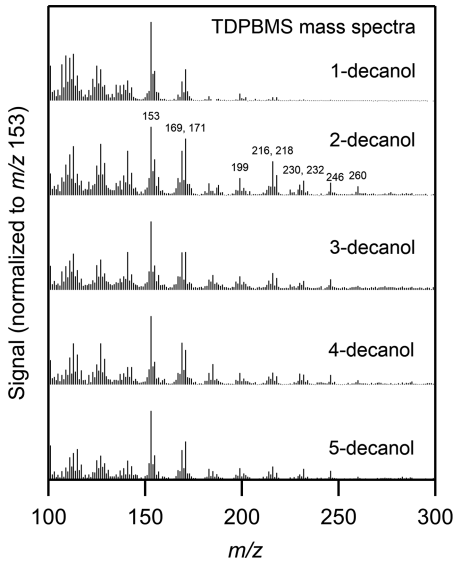

Figure 2. Real-time TDPBMS mass spectra of SOA formed from the 60 min reactions of 1-, 2-, 3-, 4-, and 5-decanol with OH radicals in the presence of NO_x. Spectra are averages for the 60 min reaction period.

(Scheme 1, Figure 1, and Table S2 of the Supporting Information). The fragmentation pathways are those we observed previously for SOA products containing the same functional groups.[27,28,35] As shown in Table 1, in most cases, product ions fragment according to the functional groups present as follows: (a) CHA (HCHA, K−CHA, CHA−N, HN−CHA, K−CHA−HC, K−N−CHA, and K−CHA−HN) loses OH; (b) HN formed through hydroxyalkoxy radical isomerization and, therefore, having a 1,4 configuration (HHN, K−HN, HN−HN, K−CHA−HN, and K−N−HN) loses NO_2 + H_2O; (c) N not part of HN (CHN−Et, HN−N, K−N−N, and K−N−HN) loses NO_3; (d) H not part of CHA or HN (HCHA and HHN) loses an additional H_2O; and (e) K not present with CHA or HN (K−N−N) loses H_2O. CHA−HC, CHHN−Et, and CHA−Es are expected to have major peaks at m/z 185, 185, and 187, but because these overlap with DOS seed particle peaks that are removed from the spectrum, their presence could not be determined.

To further probe the SOA composition, HPLC-fractionated products from the reaction of 2-decanol were collected and analyzed by CI−ITMS and ATR−FTIR. The mass spectrum of products collected at 15−30 min (Figure 3A) is shown in Figure 3B. Major peaks are observed at m/z 236, 218, and 173, which can be assigned to the $[M + H]^+$, $[M + H - H_2O]^+$, and $[M + H - HNO_3]^+$ ions formed from protonation of HHN (M = 235) and subsequent loss of H_2O and HNO_3. ATR−FTIR analysis of the same HPLC fraction yielded the spectrum shown in Figure 3C, which contains characteristic peaks as a result of hydroxyl (3360 cm^{-1}) and nitrate (1620, 1275, and 870 cm^{-1}) groups that are consistent with the HHN products.[41]

Gas-Phase Carbonyl Products. Evidence for the formation of the first-generation ketone (2-decanone) product in Scheme 1 was obtained from PTR−MS analysis during the reaction of 2-decanol. As shown in Figure 4A, soon after the reaction begins (time = 0), the signal from the $[M + H - H_2O]^+$ ion at m/z 141 that is characteristic of 2-decanol (M = 158) plummets, while at the same time, the signal at m/z 157

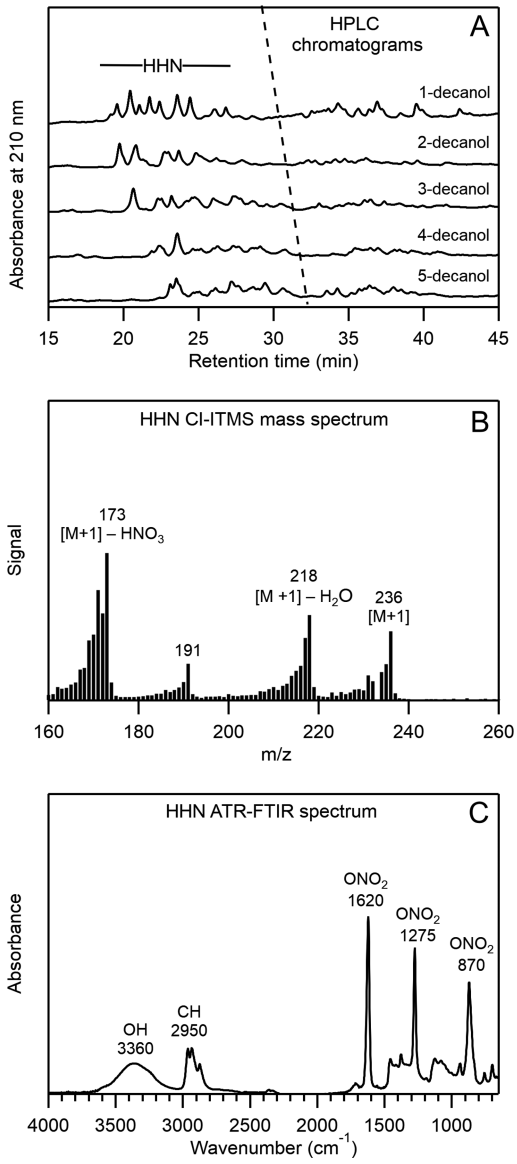

Figure 3. (A) HPLC−UV/vis chromatograms of SOA formed from the 60 min reactions of 1-, 2-, 3-, 4-, and 5-decanol with OH radicals in the presence of NO_x. Absorbance by nitrate groups was measured at 210 nm. (B) CI−ITMS mass spectrum and (C) ATR−FTIR spectrum of the HPLC HHN fraction that eluted at 15−30 min in the 2-decanol chromatogram shown in panel A.

from the $[M + H]^+$ ion of 2-decanone (M = 156) rapidly increases. As the reaction proceeds, however, the time profile of the signal from 2-decanone rolls over as a result of further reaction with OH radicals. Nonetheless, the decay is not dramatic because, in the gas phase, 2-decanone is less reactive than 2-decanol.[42]

Aldehydes formed in the reaction of 2-, 3-, and 4-decanol by decomposition of β-hydroxyalkoxy radicals were detected in GC−FID analyses. Chromatograms of the reaction products are shown in Figure 4B along with a chromatogram obtained for standards of C_6, C_7, and C_8 aldehydes (hexanal, heptanal, and octanal), which have retention times of 11.2, 13.7, and 15.7 min. According to the mechanism shown in Scheme 1, for 2-decanol one pair of aldehyde co-products (C_2 + C_8) should be formed following abstraction of a secondary H atom on the right side of the hydroxyl group, but because abstraction of a

DOI: 10.1021/acsearthspacechem.9b00015
ACS Earth Space Chem. 2019, 3, 413−423

Table 1. Mass Spectral Ion Fragments Used To Identify Reaction Products

product	generation	MW	ion fragment	neutral loss
HCHA	1	188	171	OH
			153	OH + H_2O
HHN	1	235	171	NO_2 + H_2O
			153	NO_2 + H_2O + H_2O
K−CHA	2	186	169	OH
K−HN	2	233	169	NO_2 + H_2O
CHA−N	2	233	216	OH
CHN−Et	2	233	171	NO_3
HN−CHA	2	249	232	OH
HN−N	2	280	218	NO_3
HN−HN	2	296	232	NO_2 + H_2O
K−CHA−HC	3	216	199	OH
K−N−CHA	3	247	230	OH
K−CHA−HN	3	263	246	OH
			199	NO_2 + H_2O
K−N−N	3	278	260	H_2O
			216	NO_3
K−N−HN	3	294	232	NO_3
			230	NO_2 + H_2O

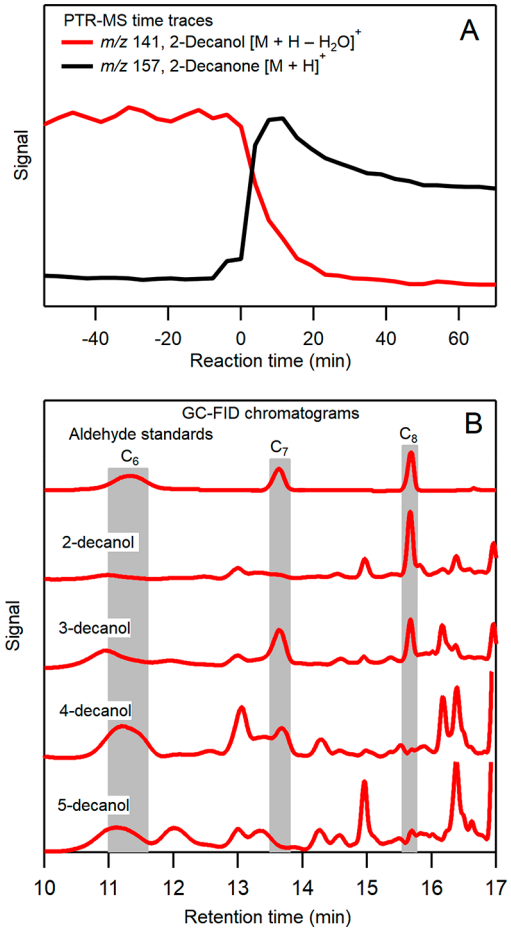

Figure 4. (A) PTR−MS time traces of 2-decanol and the 2-decanone product formed from the 60 min reaction of 2-decanol with OH radicals in the presence of NO_x. (B) GC−FID chromatograms of C_6, C_7, and C_8 aldehyde (hexanal, heptanal, and octanal) standards and products formed from the 60 min reactions of 2-, 3-, 4-, and 5-decanol with OH radicals in the presence of NO_x.

primary H atom from the left side is negligible, no significant amount of C_1 + C_9 aldehydes is expected. This is not the case for 3-, 4-, and 5-decanol, however, which have secondary H atoms on both sides of the hydroxyl group. Their reactions should each lead to the formation of two pairs of products: C_2 + C_8 and C_3 + C_7 aldehydes from 3-decanol, C_3 + C_7 and C_4 + C_6 aldehydes from 4-decanol, and C_4 + C_6 and C_5 + C_5 aldehydes from 5-decanol. Aldehydes smaller than C_6 were not detected by GC−FID analysis because cryo-cooling that was unavailable would have been necessary to obtain sufficient resolution. Nonetheless, as predicted, the C_6 aldehyde was detected in the reaction of 4- and 5-decanol, the C_7 aldehyde was detected in the reaction of 3- and 4-decanol, and the C_8 aldehyde was detected in the reaction of 2- and 3-decanol. The majority of aldehydes formed in these 1 h reactions were lost as a result of their high OH reactivity. No attempt was made to quantify their yields because corrections for losses by reaction with OH radicals would be extremely large and highly uncertain as a result of the large fraction of decanol that reacted (>90%).[43] Likewise, because the primary focus here was on SOA formation and further chemical characterization of gas-phase products would be extremely challenging, no attempt was made to identify and quantify the multifunctional products that are likely associated with the other peaks in the chromatograms.

SOA Yields. The SOA mass yields measured for the 60 min reactions of 1-, 2-, 3-, 4-, and 5-decanol were 0.518, 0.358, 0.163, 0.163, and 0.111, exhibiting a clear trend in which the yield decreases monotonically by a factor of ∼5 as the position of the hydroxyl group moves from the end to the center of the molecule. One might initially predict that this is due to a corresponding increase in isomer vapor pressures, which according to SPARC[44] calculations are 1.3, 3.8, 4.5, 4.7, and 4.7 Pa, respectively, and thus a decreasing tendency for reaction products to partition into SOA. However, although this effect may contribute to the observed trend, the differences in vapor pressures of less than a factor of 4 are too small to explain the large range in yields. For comparison, the SOA mass yields measured for C_{10} *n*-decane (this study) and C_{12} *n*-dodecane and C_{14} *n*-tetradecane (previously[16]), which have vapor pressures of 192, 15, and 1.4 Pa, were 0.152, 0.311, and 0.635. The SOA mass yields measured for reactions of the decanol isomers and these *n*-alkanes are shown in Figure 5. These linear alkanes provide a good model for evaluating the effect of precursor vapor pressure on the SOA mass yield because increasing the length of the carbon chain decreases the vapor pressures of the products but has only minor effects on the product yields. In this case, the SOA mass yields only increase by a factor of ∼4, even though the vapor pressures of the *n*-alkanes decrease by a factor of ∼140. Thus, vapor pressure alone cannot explain the trend observed in the SOA mass yields of decanol isomers, which must instead be due primarily to isomer-dependent differences in the branching ratios for the various reaction pathways shown in Scheme 1. These differences are propagated through the reactions that form first-, second-, and third-generation products, leading to major differences in the distribution of products, all of which have different vapor pressures and thus different tendencies to form SOA.

The monotonic decrease in SOA mass yields measured for the decanol isomers (and the 5- and 6-undecanol isomers, also shown in Figure 5) is similar to that observed in our previous study of SOA formation from similar reactions of a series of

DOI: 10.1021/acsearthspacechem.9b00015
ACS Earth Space Chem. 2019, 3, 413−423

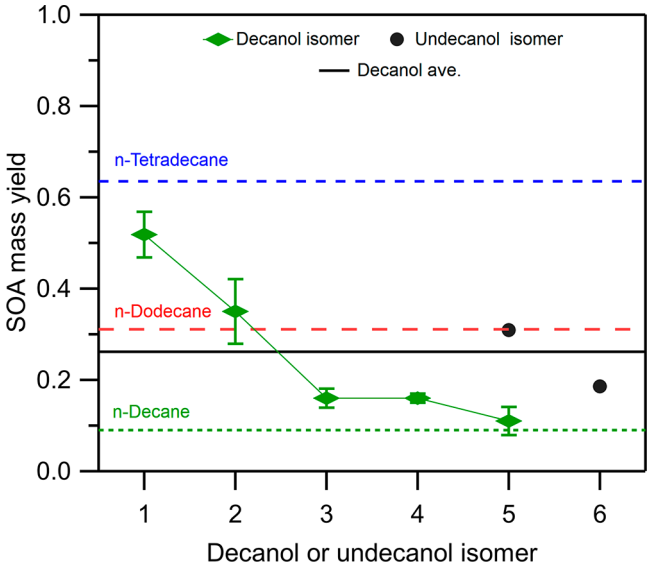

Figure 5. Mass yields of SOA formed from the 60 min reactions of 1-, 2-, 3-, 4-, and 5-decanol, 5- and 6-undecanol, and *n*-decane, *n*-dodecane, and *n*-tetradecane with OH radicals in the presence of NO_x.

dodecanone isomers,[16] although in that case, the yield increased from 5- to 6-dodecanone. Kinetics modeling indicated that this was a result of restricted rates of alkoxy radical isomerization across the keto group that led to more decomposition in the reactions of 5-dodecanone than 6-dodecanone. Unlike keto groups, hydroxyl groups are not predicted to restrict alkoxy radical isomerization,[33] and thus, a purely monotonic trend is expected. This is verified below using a similar kinetics model.

Kinetics Modeling of Isomer-Dependent Reactions. The effect of the decanol isomer structure on the SOA yield can be understood by recognizing the key role of alkoxy radical isomerization in the formation of low-volatility SOA products. As shown in Scheme 1, Figure 1, and Table 1, 12 of the 14 products that appear to be present in SOA were formed through reactions that involved alkoxy radical isomerization. The two that did not (K−N−N and HN−N) were formed by the addition of two nitrate groups to decanol or the first-generation ketone product.

A kinetics model was thus employed to determine if the fraction of first-generation products whose formation involved alkoxy radical isomerization but no decomposition could be used as a simple metric to account for the trend in measured SOA yields. The details of the model are as follows: (a) H atom abstraction by OH radicals at each site along the carbon chain was accounted for using structure−reactivity relationships;[19] (b) the branching ratio for nitrate formation was estimated to be 0.15 for reactions of all organic peroxy radicals with NO based on values reported for 1,2- and 1,4-hydroxyperoxy radicals;[39,45] (c) structure-dependent rates of alkoxy radical isomerization and decomposition were calculated using structure−activity relationships[33,34] and experimental results;[46] and (d) the rate constant for reactions of all alkoxy radicals with O_2 to form ketones and HO_2 was taken to be 3.9×10^4 s^{-1}.[47] As noted above, all first-generation products formed through alkoxy radical isomerization without subsequent decomposition (HHN and HCHA) have sufficiently low vapor pressures that they will immediately condense to form SOA. For simplicity, gas−particle and gas−wall partitioning of semi-volatile and volatile products was not included in the model nor was multi-generation chemistry. As shown in Scheme 1 and Figure 1, it is expected that second- and third-generation products will be formed by mechanisms similar to those that form first-generation products, and thus, although more SOA would be formed by including these reactions, the predicted trends with the isomer structure are unlikely to change. First-generation products were classified as decomposition (<C_{10} aldehydes), carbonyl (C_{10} ketone or aldehyde), CHA, HN, and isomerization (HCHA and HHN) products in order of highest to lowest volatility. First-generation CHA, HN, HCHA, and HHN correspond to decanol with added ketone, N, CHA, and HN groups, respectively. Note that the pathway for forming first-generation CHA only occurs following H atom abstraction at the δ-carbon and, therefore, is not shown in Scheme 1. Because this pathway is equivalent to adding a ketone group to decanol, it is not included among the isomerization products.

The product yields (moles of product formed per mole of decanol reacted) obtained from model calculations are shown in Figure 6, with the bars for each product category stacked in order of volatility. For comparison, single data points are also plotted for SOA molar yields calculated by multiplying the SOA mass yield by 158/210, the ratio of the molecular weight of decanol to the assumed average molecular weight of SOA (the average of HHN and HCHA, the two major first-generation isomerization products). The calculated yields of isomerization products, which have the lowest volatility, correlate with the SOA molar yields, whereas those of the decomposition products, which have the highest volatility, correlate inversely.

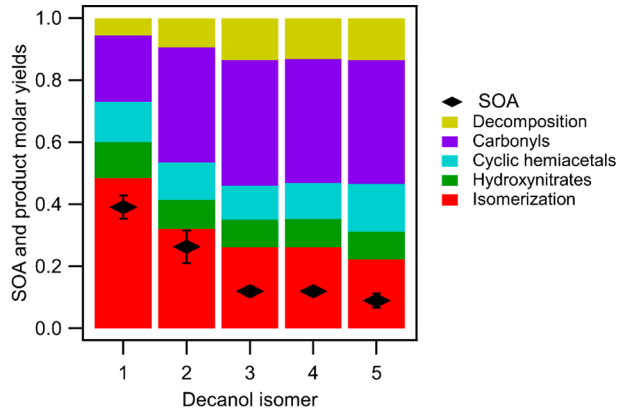

Figure 6. Molar yields of measured SOA and model-predicted first-generation products formed from the 60 min reactions of 1-, 2-, 3-, 4-, and 5-decanol with OH radicals in the presence of NO_x. Product categories are stacked from least volatile on the bottom to most volatile on the top.

Decomposition products were primarily formed following H atom abstraction at β-, γ-, or ϵ-carbons, as discussed above. Although β-hydroxyalkoxy radicals can decompose directly, γ- and ϵ-hydroxyalkoxy radicals can isomerize and then react further to form β-hydroxyalkoxy radicals, in which the alkoxy radical group is on the left and right sides of the hydroxyl group, respectively (Scheme 1), which can then decompose. Yields of C_{10} carbonyls were similar across isomers, except for 1-decanol, because abstraction of a primary H atom from the α-carbon is slower than abstraction of a secondary H atom.

DOI: 10.1021/acsearthspacechem.9b00015
ACS Earth Space Chem. 2019, 3, 413−423

Conversely, yields of HN products were slightly greater for 1-decanol compared to the other isomers (which were similar) because a greater fraction of H atom abstractions occurred at locations other than at the α-carbon, thus leading to higher yields of nitrate products. Most importantly, yields of isomerization products decreased as the hydroxyl group moved away from the end of the molecule. This was caused by enhanced H atom abstraction from α- and β-carbons in reactions with OH radicals (as a result of the greater ease of abstraction) and in alkoxy radical isomerization (as a result of shorter carbon chains), which led to higher yields of volatile carbonyls, CHA, and β-hydroxyalkoxy radical decomposition products. Thus, the yield of first-generation isomerization products shown in Figure 6 is the yield of initially formed alkoxy radicals that isomerized and did not subsequently decompose. To make more direct quantitative comparisons between measurements and model predictions, it would be necessary to include multigeneration and particle-phase reactions as well as gas−particle and gas−wall partitioning in the model.

CONCLUSION

Recent research has indicated that some of the most important compounds producing SOA from either vehicular exhaust or emissions of volatile chemical products are likely functionalized organics, which are a poorly studied class of VOCs with regards to SOA formation. The results presented here demonstrate the need to understand not only the importance of functional groups but also functional group position on VOC oxidation products and mechanisms to accurately predict SOA yields. In particular, we report on an experimental and modeling study that evaluates the effect of a hydroxyl group and its position on the SOA yields measured for the reactions of the 1-, 2-, 3-, 4-, and 5-decanol and 1- and 2-undecanol isomers with OH radicals in the presence of NO_x. Although analyses of particle composition conducted using liquid chromatography, mass spectrometry, and infrared spectroscopy indicate that the SOA formed from oxidation of each of the C_{10} decanol isomers had similar composition, the SOA yields are all enhanced relative to the yield from *n*-decane (the corresponding C_{10} *n*-alkane) and depend strongly upon the position of the functional group. When the hydroxyl group is at the end of the molecule, the SOA mass yield is a maximum of 0.5, about 5 times greater than that from *n*-decane and close to the yield from *n*-tetradecane (the C_{14} *n*-alkane). A higher yield was expected, because the addition of a hydroxyl group to *n*-decane significantly decreases the vapor pressure of the parent compound and, therefore, the vapor pressures of the products. However, as the hydroxyl group moves toward the middle of the molecule, the yield decreases monotonically to a minimum of 0.1, close to that of *n*-decane. This striking effect of the decanol isomer structure on the SOA yield occurs despite the fact that the vapor pressures only increase by about a factor of 4 from 1- to 5-decanol, whereas the vapor pressure of *n*-decane is about 2 orders of magnitude higher than that of *n*-tetradecane.

Results from a kinetic model constructed using structure−activity calculations to estimate branching ratios for major reaction pathways show that the trends in decanol SOA yields can be explained by the effect of the position of the hydroxyl group on the fraction of first-generation products formed through pathways involving alkoxy radical isomerization. These pathways tend to form low-volatility products that partition into particles, whereas the major competing pathways form more volatile products. Conclusions about the reaction mechanisms based on SOA yield measurements and modeling are supported by measurements of SOA composition, which show that the SOA mostly consists of products whose formation involves alkoxy radical isomerization. These conclusions are further supported by gas-phase measurements of the aldehyde products, because α-cleavage reactions involving β-hydroxyalkoxy radicals lead to aldehydes with carbon numbers that are specific to each decanol isomer. In general, these results are consistent with our previous study[16] on the homologous series of linear C_{12} ketone isomers reacted under similar conditions, although in that study, evidence was presented that supported the expectation (on the basis of theoretical calculations) that a keto group can hinder rates of alkoxy radical isomerization. Here, there is strong evidence that the hydroxyl group does not hinder isomerization, also in agreement with theoretical predictions.

Although this study focused on SOA formation from the reactions of monofunctional primary and secondary alcohols, a similar behavior is expected for tertiary alcohols but without formation of the first-generation ketone and with increased rates of β-hydroxyalkoxy radical decomposition because of the presence of an additional neighboring alkyl group.[33] In the case of diols, one would expect that the addition of a second hydroxyl group to a *n*-alkane backbone would have effects similar to the addition of the first hydroxyl group: an overall increase in SOA yields as a result of the lower vapor pressures of products but with a diminishing effect as the hydroxyl group moves toward the middle of the molecule because of enhanced formation of more volatile products. It is also worth noting that, although these experiments were conducted under conditions typical of polluted air, where alkylperoxy radicals react with NO, in clean air the trends are likely to be similar if the hydroxyperoxy radicals react with alkylperoxy radicals or with HO_2, because these types of reactions can also form alkoxy radicals in significant yields.[48] If reactions primarily proceed by alkylperoxy radical isomerization,[49] however, then the results would probably be quite different.

ASSOCIATED CONTENT

Supporting Information

The Supporting Information is available free of charge on the ACS Publications website at DOI: 10.1021/acsearthspacechem.9b00015.

> Major products formed from the reaction of decanol with OH radicals in the presence of NO_x (Table S1) and their vapor pressures calculated using SIMPOL.1 and fraction of each product that is predicted to partition to the particles at different aerosol mass loadings (Table S2) (PDF)

AUTHOR INFORMATION

Corresponding Author

*E-mail: paul.ziemann@colorado.edu.

ORCID

Paul J. Ziemann: 0000-0001-7419-0044

Notes

The authors declare no competing financial interest.

DOI: 10.1021/acsearthspacechem.9b00015
ACS Earth Space Chem. 2019, 3, 413−423

■ ACKNOWLEDGMENTS

This material is based on work supported by the National Science Foundation (NSF) under Grants AGS-1420007 and AGS-1750447.

■ REFERENCES

(1) World Meteorological Organization (WMO). *Scientific Assessment of Ozone Depletion: 2014*; WMO: Geneva, Switzerland, February 1995; Report 37.

(2) Ziemann, P. J.; Atkinson, R. Kinetics, Products, and Mechanisms of Secondary Organic Aerosol Formation. *Chem. Soc. Rev.* **2012**, *41*, 6582−6605.

(3) Zhang, Q.; Jimenez, J. L.; Canagaratna, M. R.; Allan, J. D.; Coe, H.; Ulbrich, I.; Alfarra, M. R.; Takami, A.; Middlebrook, A. M.; Sun, Y. L.; Dzepina, K.; Dunlea, E.; Docherty, K.; DeCarlo, P. F.; Salcedo, D.; Onasch, T.; Jayne, J. T.; Miyoshi, T.; Shimono, A.; Hatakeyama, S.; Takegawa, N.; Kondo, Y.; Schneider, J.; Drewnick, F.; Borrmann, S.; Weimer, S.; Demerjian, K.; Williams, P.; Bower, K.; Bahreini, R.; Cottrell, L.; Griffin, R. J.; Rautiainen, J.; Sun, J. Y.; Zhang, Y. M.; Worsnop, D. R. Ubiquity and Dominance of Oxygenated Species in Organic Aerosols in Anthropogenically-Influenced Northern Hemisphere Midlatitudes. *Geophys. Res. Lett.* **2007**, *34*, L13801.

(4) Pöschl, U. Atmospheric Aerosols: Composition, Transformation, Climate and Health Effects. *Angew. Chem., Int. Ed.* **2005**, *44*, 7520−7540.

(5) McDonald, B. C.; Goldstein, A. H.; Harley, R. A. Long-Term Trends in California Mobile Source Emissions and Ambient Concentrations of Black Carbon and Organic Aerosol. *Environ. Sci. Technol.* **2015**, *49*, 5178−5188.

(6) Gentner, D. R.; Jathar, S. H.; Gordon, T. D.; Bahreini, R.; Day, D. A.; El Haddad, I.; Hayes, P. L.; Pieber, S. M.; Platt, S. M.; de Gouw, J.; Goldstein, A. H.; Harley, R. A.; Jimenez, J. L.; Prévôt, A. S. H.; Robinson, A. L. Review of Urban Secondary Organic Aerosol Formation from Gasoline and Diesel Motor Vehicle Emissions. *Environ. Sci. Technol.* **2017**, *51*, 1074−1093.

(7) Gentner, D. R.; Isaacman, G.; Worton, D. R.; Chan, A. W. H.; Dallmann, T. R.; Davis, L.; Liu, S.; Day, D. A.; Russell, L. M.; Wilson, K. R.; Weber, R.; Guha, A.; Harley, R. A.; Goldstein, A. H. Elucidating Secondary Organic Aerosol from Diesel and Gasoline Vehicles through Detailed Characterization of Organic Carbon Emissions. *Proc. Natl. Acad. Sci. U. S. A.* **2012**, *109*, 18318−18323.

(8) Jathar, S. H.; Gordon, T. D.; Hennigan, C. J.; Pye, H. O. T.; Pouliot, G.; Adams, P. J.; Donahue, N. M.; Robinson, A. L. Unspeciated Organic Emissions from Combustion Sources and their Influence on the Secondary Organic Aerosol Budget in the United States. *Proc. Natl. Acad. Sci. U. S. A.* **2014**, *111*, 10473−10478.

(9) McDonald, B. C.; de Gouw, J. A.; Gilman, J. B.; Jathar, S. H.; Akherati, A.; Cappa, C. D.; Jimenez, J. L.; Lee-Taylor, J.; Hayes, P. L.; McKeen, S. A.; Cui, Y. Y.; Kim, S.-W.; Gentner, D. R.; Isaacman-VanWertz, G.; Goldstein, A. H.; Harley, R. A.; Frost, G. J.; Roberts, J. M.; Ryerson, T. B.; Trainer, M. Volatile Chemical Products Emerging as Largest Petrochemical Source of Urban Organic Emissions. *Science* **2018**, *359*, 760−764.

(10) Warneke, C.; de Gouw, J. A.; Holloway, J. S.; Peischl, J.; Ryerson, T. B.; Atlas, E.; Blake, D.; Trainer, M.; Parrish, D. D. Multiyear Trends in Volatile Organic Compounds in Los Angeles, California: Five Decades of Decreasing Emissions. *J. Geophys. Res.: Atmos.* **2012**, *117* (D21), D00V17.

(11) Papagni, C.; Arey, J.; Atkinson, R. Rate Constants for the Gas-Phase Reactions of OH Radicals with a Series of Unsaturated Alcohols. *Int. J. Chem. Kinet.* **2001**, *33*, 142−147.

(12) Reisen, F.; Aschmann, S. M.; Atkinson, R.; Arey, J. Hydroxyaldehyde Products from Hydroxyl Radical Reactions of Z-3-Hexen-1-ol and 2-Methyl-3-Buten-2-ol Quantified by SPME and API-MS. *Environ. Sci. Technol.* **2003**, *37*, 4664−4671.

(13) McGillen, M. R.; Tyndall, G. S.; Orlando, J. J.; Pimentel, A. S.; Medeiros, D. J.; Burkholder, J. B. Experimentally Determined Site-Specific Reactivity of the Gas-Phase OH and Cl + *i*-Butanol Reactions Between 251 and 340 K. *J. Phys. Chem. A* **2016**, *120*, 9968−9981.

(14) Le Person, A.; Solignac, G.; Oussar, F.; Daele, V.; Mellouki, A.; Winterhalter, R.; Moortgat, G. K. Gas Phase Reaction of Allyl Alcohol (2-Propen-1-ol) with OH Radicals and Ozone. *Phys. Chem. Chem. Phys.* **2009**, *11*, 7619−7628.

(15) Li, W.; Li, L.; Chen, C.; Kacarab, M.; Peng, W.; Price, D.; Xu, J.; Cocker, D. R., III The Potential of Select Intermediate-Volatility Organic Compounds (IVOCs) and, Consumer Products for Secondary Organic Aerosol (SOA) and Ozone Formation Under Relevant Urban Conditions. *Atmos. Environ.* **2018**, *178*, 109−117.

(16) Algrim, L. B.; Ziemann, P. J. Effect of the Keto Group on Yields and Composition of Organic Aerosol Formed from OH Radical-Initiated Reactions of Ketones in the Presence of NO_x. *J. Phys. Chem. A* **2016**, *120*, 6978−6989.

(17) Taylor, W. D.; Allston, T. D.; Moscato, M. J.; Fazekas, G. B.; Kozlowski, R.; Takacs, G. A. Atmospheric Photodissociation Lifetimes for Nitromethane, Methyl Nitrite, and Methyl Nitrate. *Int. J. Chem. Kinet.* **1980**, *12*, 231−240.

(18) Atkinson, R.; Carter, W. P. L.; Winer, A. M.; Pitts, J. N. An Experimental Protocol for the Determination of OH Radical Rate Constants with Organics using Methyl Nitrite Photolysis as an OH Radical Source. *J. Air Pollut. Control Assoc.* **1981**, *31*, 1090−1092.

(19) Ziemann, P. J.; Atkinson, R. Kinetics, Products, and Mechanisms of Secondary Organic Aerosol Formation. *Chem. Soc. Rev.* **2012**, *41*, 6582−6605.

(20) de Gouw, J.; Warneke, C. Measurements of Volatile Organic Compounds in the Earth's Atmosphere using Proton-Transfer-Reaction Mass Spectrometry. *Mass Spectrom. Rev.* **2007**, *26*, 223−257.

(21) Tobias, H. J.; Kooiman, P. M.; Docherty, K. S.; Ziemann, P. J. Real-Time Chemical Analysis of Organic Aerosols Using a Thermal Desorption Particle Beam Mass Spectrometer. *Aerosol Sci. Technol.* **2000**, *33*, 170−190.

(22) Docherty, K.; Ziemann, P. Effects of Stabilized Criegee Intermediate and OH Radical Scavengers on Aerosol Formation from Reactions of β-Pinene with O_3. *Aerosol Sci. Technol.* **2003**, *37*, 877−891.

(23) Ranney, A. P.; Ziemann, P. J. Identification and Quantification of Oxidized Organic Aerosol Compounds Using Derivatization, Liquid Chromatography, and Chemical Ionization Mass Spectrometry. *Aerosol Sci. Technol.* **2017**, *51*, 342−353.

(24) Odum, J. R.; Hoffmann, T.; Bowman, F.; Collins, D.; Flagan, R. C.; Seinfeld, J. H. Gas/Particle Partitioning and Secondary Organic Aerosol Yields. *Environ. Sci. Technol.* **1996**, *30*, 2580−2585.

(25) Lim, Y. B.; Ziemann, P. J. Effects of Molecular Structure on Aerosol Yields from OH Radical-Initiated Reactions of Linear, Branched, and Cyclic Alkanes in the Presence of NO_x. *Environ. Sci. Technol.* **2009**, *43*, 2328−2334.

(26) Wang, N.; Jorga, S. D.; Pierce, J. R.; Donahue, N. M.; Pandis, S. N. Particle Wall-Loss Correction Methods in Smog Chamber Experiments. *Atmos. Meas. Tech.* **2018**, *11*, 6577−6588.

(27) Yeh, G. K.; Ziemann, P. J. Gas-Wall Partitioning of Oxygenated Organic Compounds: Measurements, Structure-Activity Relationships, and Correlation with Gas Chromatographic Retention Factor. *Aerosol Sci. Technol.* **2015**, *49*, 727−738.

(28) Yeh, G. K.; Ziemann, P. J. Alkyl Nitrate Formation from the Reactions of C_8−C_{14} *n*-Alkanes with OH Radicals in the Presence of NO_x. *J. Phys. Chem. A* **2014**, *118*, 8147−−8157.

(29) Matsunaga, A.; Ziemann, P. J. Gas-Wall Partitioning of Organic Compounds in a Teflon Film Chamber and Potential Effects on Reaction Product and Aerosol Yield Measurements. *Aerosol Sci. Technol.* **2010**, *44*, 881−892.

(30) Krechmer, J. E.; Pagonis, D.; Ziemann, P. J.; Jimenez, J. L. Quantification of Gas-Wall Partitioning in Teflon Environmental Chambers Using Rapid Bursts of Low-Volatility Oxidized Species Generated in Situ. *Environ. Sci. Technol.* **2016**, *50*, 5757−5765.

(31) McVay, R. C.; Cappa, C. D.; Seinfeld, J. H. Vapor-Wall Deposition in Chambers: Theoretical Considerations. *Environ. Sci. Technol.* **2014**, *48*, 10251−1025.

DOI: 10.1021/acsearthspacechem.9b00015
ACS Earth Space Chem. 2019, 3, 413−423

(32) Bethel, H. L.; Atkinson, R.; Arey, J. Kinetics and Products of the Reactions of Selected Diols with the OH Radical. *Int. J. Chem. Kinet.* **2001**, *33*, 310−316.
(33) Vereecken, L.; Peeters, J. Decomposition of Substituted Alkoxy Radicals-Part I: A Generalized Structure-Activity Relationship for Reaction Barrier Heights. *Phys. Chem. Chem. Phys.* **2009**, *11*, 9062−9074.
(34) Vereecken, L.; Peeters, J. A Structure-Activity Relationship for the Rate Coefficient of H-Migration in Substituted Alkoxy Radicals. *Phys. Chem. Chem. Phys.* **2010**, *12*, 12608−12620.
(35) Lim, Y. B.; Ziemann, P. J. Chemistry of Secondary Organic Aerosol Formation from OH Radical-Initiated Reactions of Linear, Branched, and Cyclic Alkanes in the Presence of NO_x. *Aerosol Sci. Technol.* **2009**, *43*, 604−619.
(36) Ranney, A. P.; Ziemann, P. J. Kinetics of Acid-Catalyzed Dehydration of Cyclic Hemiacetals in Organic Aerosol Particles in Equilibrium with Nitric Acid Vapor. *J. Phys. Chem. A* **2016**, *120*, 2561−2568.
(37) Pankow, J. F.; Asher, W. E. SIMPOL.1: A Simple Group Contribution Method for Predicting Vapor Pressures and Enthalpies of Vaporization of Multifunctional Organic Compounds. *Atmos. Chem. Phys.* **2008**, *8*, 2773−2796.
(38) Pankow, J. F. An Absorption Model of the Gas/Aerosol Partitioning of Organic Compounds in the Atmosphere. *Atmos. Environ.* **1994**, *28*, 185−188.
(39) Matsunaga, A.; Ziemann, P. J. Yields of β-Hydroxynitrates and Dihydroxynitrates in Aerosol Formed from OH Radical-Initiated Reactions of Linear Alkenes in the Presence of NO_x. *J. Phys. Chem. A* **2009**, *113*, 599−606.
(40) McLafferty, F. W.; Turecek, F. *Interpretation of Mass Spectra*, 4th ed.; University Science Books: Sausalito, CA, 1993.
(41) Day, D. A.; Liu, S.; Russell, L. M.; Ziemann, P. J. Organonitrate Group Concentrations in Submicron Particles with High Nitrate and Organic Fractions in Coastal Southern California. *Atmos. Environ.* **2010**, *44*, 1970−1979.
(42) Atkinson, R.; Arey, J. Atmospheric Degradation of Volatile Organic Compounds. *Chem. Rev.* **2003**, *103*, 4605−4638.
(43) Atkinson, R.; Aschmann, S. M.; Carter, W. P. L.; Winer, A. M.; Pitts, J. N. Alkyl Nitrate Formation from the NO_x-Air Photooxidations of C_2−C_8 *n*-Alkanes. *J. Phys. Chem.* **1982**, *86*, 4563−4569.
(44) Hilal, S. H.; Karickhoff, S. W.; Carreira, L. A. Prediction of the Vapor Pressure, Boiling Point, Heat of Vaporization and Diffusion Coefficient of Organic Compounds. *QSAR Comb. Sci.* **2003**, *22*, 565−574.
(45) Yeh, G. K.; Ziemann, P. J. Identification and Yields of 1,4-Hydroxynitrates Formed from the Reactions of C_8−C_{16} *n*-Alkanes with OH Radicals in the Presence of NO_x. *J. Phys. Chem. A* **2014**, *118*, 8797−8806.
(46) Aschmann, S. M.; Tuazon, E. C.; Arey, J.; Atkinson, R. Products and Mechanisms of the Gas-Phase Reactions of OH Radicals with 1-Octene and 7-Tetradecene in the Presence of NO. *Environ. Sci. Technol.* **2010**, *44*, 3825−3831.
(47) Atkinson, R. Rate Constants for the Atmospheric Reactions of Alkoxy Radicals: An Updated Estimation Method. *Atmos. Environ.* **2007**, *41*, 8468−8485.
(48) Orlando, J. J.; Tyndall, G. S. Laboratory Studies of Organic Peroxy Radical Chemistry: An Overview with Emphasis on Recent Issues of Atmospheric Significance. *Chem. Soc. Rev.* **2012**, *41*, 6294−6317.
(49) Crounse, J. D.; Nielsen, L. B.; Jørgensen, S.; Kjaergaard, H. G.; Wennberg, P. O. Autoxidation of Organic Compounds in the Atmosphere. *J. Phys. Chem. Lett.* **2013**, *4*, 3513−3520.

DOI: 10.1021/acsearthspacechem.9b00015
ACS Earth Space Chem. 2019, 3, 413−423

Supporting Information

Effect of the Hydroxyl Group on Yields and Composition of Organic Aerosol Formed from OH Radical-Initiated Reactions of Alcohols in the Presence of NOx

Lucas B. Algrim[†,‡], Paul J. Ziemann[†,‡]

Department of Chemistry and Biochemistry, and Cooperative Institute for Research in Environmental Sciences (CIRES), Boulder, Colorado 80309

† Cooperative Institute for Research in Environmental Sciences (CIRES), Boulder, Colorado 80309, United States

‡ Department of Chemistry and Biochemistry, University of Colorado, Boulder, Colorado 80309,
United States

Abstract., The fraction of OH reaction at each carbon of each decanol isomer (Table S1), and decanol oxidation product vapor pressures and resulting percent in the particle phase at various particle loadings (Table S2).

Table S1. Table showing fraction of initial OH abstraction from each carbon for every decanol isomer, as predicted by the estimation methods.[3] It is shown that the most reactive carbon is always the α-carbon (red) followed by the β-carbon (orange). Decreased reactivity of the α-carbon in 1-decanol is due it being primary, versus the secondary α-carbon in the 2-5 decanol isomers.

	1-decano1	2-decanol	3-decanol	4-decanol	5-decanol
C_1	21%	2%	1%	1%	1%
C_2	16%	37%	12%	5%	5%
C_3	9%	16%	40%	14%	7%
C_4	9%	8%	14%	40%	14%
C_5	9%	8%	7%	14%	40%
C_6	9%	8%	7%	7%	14%
C_7	9%	8%	7%	7%	7%
C_8	9%	8%	7%	7%	7%
C_9	7%	6%	5%	5%	5%
C_{10}	1%	1%	1%	1%	1%

Table S2. Estimated vapor pressure (at 298 K) and percent-in-particle of decanol and its first-, second-, and third-generation oxidation products at varying particle loadings as determined by SIMPOL.1 vapor pressure prediction[1] and gas-particle partitioning theory.[2]

			% in particle at given mass loading (μg m^{-3})			
Compound	Gen.	ρ^o (atm)	**500**	**1000**	**1500**	**2000**
decanol	–	1.56E-05	1%	1%	2%	2%
decanone	1	2.81E-04	0%	0%	0%	0%
HN	1	1.06E-07	48%	65%	73%	79%
HHN	1	6.07E-10	99%	100%	100%	100%
HHC	1	9.19E-09	91%	96%	97%	98%
HCHA	1	1.96E-08	83%	91%	94%	95%
HDHF	1	2.37E-06	2%	4%	6%	8%
HC	1	1.61E-06	6%	11%	15%	20%
CHA	1	3.43E-06	3%	5%	8%	10%
DHF	1	4.14E-04	0%	0%	0%	0%
K-N	2	1.90E-06	5%	9%	13%	17%
K-HN	2	1.09E-08	90%	95%	96%	97%
K-CHA	2	3.50E-07	22%	36%	46%	53%
HN-N	2	7.17E-10	99%	100%	100%	100%
HN-HN	2	4.10E-12	100%	100%	100%	100%
HN-CHA	2	1.30E-10	100%	100%	100%	100%
CHA-N	2	2.32E-08	81%	89%	93%	94%
CHN-Et	2	2.32E-08	81%	89%	93%	94%
HCHN-Et	2	1.33E-10	100%	100%	100%	100%
CHA-HC	2	2.01E-09	98%	99%	99%	99%
C-Es	2	1.58E-05	1%	1%	2%	2%
CHA-Es	2	2.32E-07	30%	46%	56%	63%
K-N-N	3	1.28E-08	88%	94%	96%	97%
K-N-CHA	3	2.37E-09	98%	99%	99%	99%
K-N-HN	3	7.34E-11	100%	100%	100%	100%
K-CHA-HN	3	1.36E-11	100%	100%	100%	100%
K-CHA-HC	3	2.05E-10	100%	100%	100%	100%

REFERENCES

1. Pankow, J. F.; Asher, W. E. SIMPOL.1: A Simple Group Contribution Method for Predicting Vapor Pressures and Enthalpies of Vaporization of Multifunctional Organic Compounds. *Atmos. Chem. Phys*. **2008**, *8*, 2773–2796.

2. Pankow, J. F. An Absorption Model of the Gas/Aerosol Partitioning of Organic Compounds in the Atmosphere. *Atmos*. *Environ*. **1994**, *28*, 185–188.

3. Ziemann, P. J.; Atkinson, R. Kinetics, Products, and Mechanisms of Secondary Organic Aerosol Formation. *Chem. Soc. Rev*. **2012**, *41*, 6582−6605.